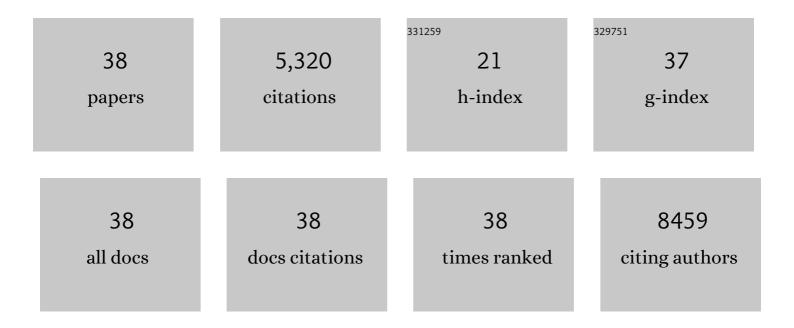
Brian C Olsen

List of Publications by Year in descending order

Source: https://exaly.com/author-pdf/2278636/publications.pdf Version: 2024-02-01



#	Article	IF	CITATIONS
1	Bipolar Resistive Switching in Junctions of Gallium Oxide and p-type Silicon. Nano Letters, 2021, 21, 2666-2674.	4.5	24
2	Solvent Vapor Annealing, Defect Analysis, and Optimization of Self-Assembly of Block Copolymers Using Machine Learning Approaches. ACS Applied Materials & Interfaces, 2021, 13, 28639-28649.	4.0	12
3	Kinetics of Plasmon-Driven Hydrosilylation of Silicon Surfaces: Photogenerated Charges Drive Silicon–Carbon Bond Formation. Journal of Physical Chemistry C, 2021, 125, 17983-17992.	1.5	0
4	Beyond Thin Films: Clarifying the Impact of <i>c</i> -Li ₁₅ Si ₄ Formation in Thin Film, Nanoparticle, and Porous Si Electrodes. ACS Applied Materials & Interfaces, 2021, 13, 38147-38160.	4.0	4
5	Optimization of the Bulk Heterojunction of All-Small-Molecule Organic Photovoltaics Using Design of Experiment and Machine Learning Approaches. ACS Applied Materials & Interfaces, 2020, 12, 54596-54607.	4.0	22
6	Stabilizing Tin Anodes in Sodium-Ion Batteries by Alloying with Silicon. ACS Applied Energy Materials, 2020, 3, 9950-9962.	2.5	23
7	van der Waals Epitaxy of Soft Twisted Bilayers: Lattice Relaxation and Mass Density Waves. ACS Nano, 2020, 14, 13441-13450.	7.3	8
8	Redox Flow Batteries: How to Determine Electrochemical Kinetic Parameters. ACS Nano, 2020, 14, 2575-2584.	7.3	118
9	Water-soluble pH-switchable cobalt complexes for aqueous symmetric redox flow batteries. Chemical Communications, 2020, 56, 3605-3608.	2.2	9
10	Adhesion and Surface Layers on Silicon Anodes Suppress Formation of <i>c</i> -Li _{3.75} Si and Solid-Electrolyte Interphase. ACS Applied Energy Materials, 2020, 3, 1609-1616.	2.5	10
11	Understanding the Mechanism of Enhanced Cycling Stability in Sn–Sb Composite Na-Ion Battery Anodes: Operando Alloying and Diffusion Barriers. ACS Applied Energy Materials, 2019, 2, 5133-5139.	2.5	14
12	Alternating Silicon and Carbon Multilayer-Structured Anodes Suppress Formation of the c-Li _{3.75} Si Phase. Chemistry of Materials, 2019, 31, 6578-6589.	3.2	19
13	Plasmonic Stamps Fabricated by Gold Dewetting on PDMS for Catalyzing Hydrosilylation on Silicon Surfaces. ACS Applied Nano Materials, 2019, 2, 3238-3245.	2.4	8
14	Sb–Si Alloys and Multilayers for Sodium-Ion Battery Anodes. ACS Applied Energy Materials, 2019, 2, 2205-2213.	2.5	52
15	UV-Initiated Si–S, Si–Se, and Si–Te Bond Formation on Si(111): Coverage, Mechanism, and Electronics. Journal of Physical Chemistry C, 2018, 122, 13803-13814.	1.5	25
16	Vapor-Phase Nanopatterning of Aminosilanes with Electron Beam Lithography: Understanding and Minimizing Background Functionalization. Langmuir, 2018, 34, 4780-4792.	1.6	8
17	How To Optimize Materials and Devices <i>via</i> Design of Experiments and Machine Learning: Demonstration Using Organic Photovoltaics. ACS Nano, 2018, 12, 7434-7444.	7.3	219
18	β-SnSb for Sodium Ion Battery Anodes: Phase Transformations Responsible for Enhanced Cycling Stability Revealed by In Situ TEM. ACS Energy Letters, 2018, 3, 1670-1676.	8.8	90

BRIAN C OLSEN

#	Article	IF	CITATIONS
19	Preferential Alignment of Incommensurate Block Copolymer Dot Arrays Forming Moiré Superstructures. ACS Nano, 2017, 11, 3237-3246.	7.3	21
20	Sn–Bi–Sb alloys as anode materials for sodium ion batteries. Journal of Materials Chemistry A, 2017, 5, 9661-9670.	5.2	124
21	Understanding the Effects of a High Surface Area Nanostructured Indium Tin Oxide Electrode on Organic Solar Cell Performance. ACS Applied Materials & Interfaces, 2017, 9, 38706-38715.	4.0	14
22	Nanopatterning via Solvent Vapor Annealing of Block Copolymer Thin Films. Chemistry of Materials, 2017, 29, 176-188.	3.2	94
23	Sequential Nanopatterned Block Copolymer Self-Assembly on Surfaces. Langmuir, 2016, 32, 5890-5898.	1.6	17
24	Polymers, Plasmons, and Patterns: Mechanism of Plasmon-Induced Hydrosilylation on Silicon. Chemistry of Materials, 2016, 28, 9158-9168.	3.2	13
25	Substance over Subjectivity: Moving beyond the Histogram. Chemistry of Materials, 2016, 28, 5973-5975.	3.2	21
26	Role of Interfacial Layers in Organic Solar Cells: Energy Level Pinning versus Phase Segregation. ACS Applied Materials & Interfaces, 2016, 8, 18238-18248.	4.0	57
27	Nanoscale Plasmonic Stamp Lithography on Silicon. ACS Nano, 2015, 9, 2184-2193.	7.3	25
28	Hybrid Device Employing Three-Dimensional Arrays of MnO in Carbon Nanosheets Bridges Battery–Supercapacitor Divide. Nano Letters, 2014, 14, 1987-1994.	4.5	276
29	Nickel/Iron Oxide Nanocrystals with a Nonequilibrium Phase: Controlling Size, Shape, and Composition. Chemistry of Materials, 2014, 26, 4796-4804.	3.2	34
30	Carbon Nanosheet Frameworks Derived from Peat Moss as High Performance Sodium Ion Battery Anodes. ACS Nano, 2013, 7, 11004-11015.	7.3	813
31	Mesoporous nitrogen-rich carbons derived from protein for ultra-high capacity battery anodes and supercapacitors. Energy and Environmental Science, 2013, 6, 871.	15.6	983
32	Interconnected Carbon Nanosheets Derived from Hemp for Ultrafast Supercapacitors with High Energy. ACS Nano, 2013, 7, 5131-5141.	7.3	869
33	Graphene-nickel cobaltite nanocomposite asymmetrical supercapacitor with commercial level mass loading. Nano Research, 2012, 5, 605-617.	5.8	356
34	Carbonized Chicken Eggshell Membranes with 3D Architectures as Highâ€Performance Electrode Materials for Supercapacitors. Advanced Energy Materials, 2012, 2, 431-437.	10.2	573
35	Carbonized Chicken Eggshell Membranes with 3D Architectures as High-Performance Electrode Materials for Supercapacitors (Adv. Energy Mater. 4/2012). Advanced Energy Materials, 2012, 2, 430-430.	10.2	10
36	High Rate Electrochemical Capacitors from Three-Dimensional Arrays of Vanadium Nitride Functionalized Carbon Nanotubes. Journal of Physical Chemistry C, 2011, 115, 24381-24393.	1.5	145

#	Article	IF	CITATIONS
37	Supercapacitive Properties of Hydrothermally Synthesized Co ₃ O ₄ Nanostructures. Journal of Physical Chemistry C, 2011, 115, 17599-17605.	1.5	179
38	Solid-state dewetting mechanisms of ultrathin Ni films revealed by combining <i>in situ</i> time resolved differential reflectometry monitoring and atomic force microscopy. Physical Review B, 2010, 82, .	1.1	31